Journal of Materials Chemistry A

Stabilization of a high H^--conducting phase via K doping of Ba-Li oxyhydride

Journal:	*Journal of Materials Chemistry A*
Manuscript ID	TA-COM-08-2022-006278.R1
Article Type:	Communication
Date Submitted by the Author:	03-Oct-2022
Complete List of Authors:	Okamoto, Kei; National Institutes of Natural Sciences - Okazaki Campus, Institute for Molecular Science; Takeiri, Fumitaka; Institute for Molecular Science, Department of Materials Molecular Science Imai, Yumiko; Institute for Molecular Science, Department of Materials Molecular Science Yonemura, Masao; High Energy Accelerator Research Organization Saito, Takashi; High Energy Accelerator Research Organization, Institute of Materials Structure Science; The Graduate University for Advanced Studies, School of High Energy Accelerator Science Ikeda, Kazutaka; High Energy Accelerator Reserch Organization, Insititute of Materials Structure Science Otomo, Toshiya; High Energy Accelerator Research Organization Kamiyama, Takashi ; High Energy Accelerator Research Organization Kobayashi, Genki; RIKEN, Cluster for Pioneering Research

COMMUNICATION

Stabilization of a high H^--conducting phase via K doping of Ba-Li oxyhydride

Received 00th January 20xx,
Accepted 00th January 20xx

DOI: 10.1039/x0xx00000x

Kei Okamoto,[abc] Fumitaka Takeiri,[abcd] Yumiko Imai,[c] Masao Yonemura,[ef] Takashi Saito,[ef] Kazutaka Ikeda,[ef] Toshiya Otomo,[ef] Takashi Kamiyama [ef] and Genki Kobayashi *[ab]

We report the aliovalent partial substitution of Ba with K in Ba-Li oxyhydride, which exhibits a high H^- conductivity caused by structural phase transitions. The phase transition temperatures were decreased by approximately 50 °C via 15% K/Ba substitution, resulting in a high conductivity at lower temperatures.

Structural phase transitions are a critical research topic in the field of crystalline solids, and their tuning via elemental substitution is key in the emergence of functions. Particularly, in ion conductors, a high-temperature phase with a higher-symmetry lattice generally favors fast ion conduction, such as AgI[1] and $Ba_2In_2O_5$.[2] In AgI, a transition from a hexagonal β-phase to a cubic α-phase at 146 °C induces a Ag^+ superionic conduction state, whereas in $Ba_2In_2O_5$, a transition from a brownmillerite to a perovskite structure yields fast O^{2-} conduction at >925 °C. A well-known strategy to stabilize such a fast conduction phase is the introduction of structural randomness via elemental substitution or solid solution formation. In AgI, partial Br^-/I^- substitution decreases the critical point,[3] and furthermore, the introduction of Rb^+ into the system yields $RbAg_4I_5$ with a stabilized cubic lattice upon cooling to room temperature.[4] Elemental substitution in $Ba_2In_2O_5$, yielding products such as $(Ba,La)_2In_2O_5$[5] and $Ba_2(In,Ga)_2O_5$,[6] is also effective in stabilizing the perovskite lattice.

[a] Solid State Chemistry Laboratory, Cluster for Pioneering Research (CPR), RIKEN, Wako 351-0198, Japan.
[b] Department of Materials Molecular Science, Institute for Molecular Science, Okazaki 444-8585, Japan.
[c] Department of Structural Molecular Science, School of Physical Sciences, SOKENDAI (The Graduate University for Advanced Studies), Okazaki 444-8585, Japan.
[d] Japan Science and Technology Agency (JST), Precursory Research for Embryonic Science and Technology (PRESTO), 4-1-8 Honcho, Kawaguchi, Saitama 332-0012, Japan
[e] Institute of Materials Structure Science, High Energy Accelerator Research Organization (KEK), Ibaraki 305-0801, Japan
[f] Department of Materials Structure Science, School of High Energy Accelerator Science, SOKENDAI (The Graduate University for Advanced Studies), Ibaraki 305-0801, Japan

† Footnotes relating to the title and/or authors should appear here.
Electronic Supplementary Information (ESI) available: [details of any supplementary information available should be included here]. See DOI: 10.1039/x0xx00000x

Hydride ion (H^-) conductors are an emerging class in the field of solid state ionics. The monovalent, soft H^- is a promising charge carrier in electrochemical hydrogen use, particularly at intermediate temperatures (200–400 °C), which is impossible using proton conductors. Alkaline-earth hydrides AEH_2 (*AE* = Ca, Sr, and Ba)[7, 8] and oxyhydrides $La_{2-x-y}Sr_{x+y}LiH_{1-x+y}O_{3-y}$[9] reported in around 2015 may be regarded as the early stage of this research field. Subsequently, various materials were discovered, e.g., K_2NiF_4-type Ln_2LiHO_3 (*Ln* = La, Pr, and Nd)[10] and Ba_2MHO_3 (*M* = Sc[11] and Y[12]), fluorite oxyhydrides $LnH_{3-x}O_x$ (*Ln* = La and Nd),[13-16] layered hydride-halides Ba_2H_3X (*X* = Cl, Br, and I),[17, 18] and perovskite hydrides $AELiH_3$ (*AE* = Ca, Sr, and Ba),[19] along with theoretical investigations of H^- conduction.[20-23] However, notable conductivity at intermediate temperatures is severely limited in $LaH_{2.52}O_{0.24}$ (2.6×10^{-2} S·cm^{-1} at 342 °C)[13] and Ba_2H_3I (>10^{-3} S·cm^{-1} at 200–300 °C), and further material investigations remain challenging.

We recently reported K_2NiF_4-type Ba-Li oxyhydrides (BLHOs), including $Ba_2LiH_{2.8}O_{1.1}$ synthesized using a high-pressure method (α-BLHO) and $Ba_{1.75}LiH_{2.7}O_{0.9}$ (β-BLHO), which is the stable composition under ambient pressure.[24] At room temperature, β-BLHO exhibits an orthorhombic unit cell with three types of long-range order at the Ba, equatorial H, and apical sites. Upon heating, the former two melt at 300 °C, with the orthorhombic lattice (γ-BLHO) remaining, followed by a transformation at 360 °C to a tetragonal lattice (δ-BLHO), with the long-range order no longer observed. These successive order/disorder transitions induce a high, almost temperature-independent H^- conductivity of >10^{-2} S·cm^{-1}. The introduction of structural randomness into BLHO via elemental substitutions should stabilize the γ- and δ-phases at lower temperatures. In this study, we selected K^+, which has weak electrostatic interactions due to a monovalence and is comparable in size to Ba^{2+} as the substituent species and demonstrated the partial substitution of Ba with K in BLHO and its effects on the structural phase transitions and H^- conductivity.

Powder samples with nominal compositions of $Ba_{2-x}K_xLiH_{3-x}O$ (*x* = 0.1, 0.2, or 0.3), denoted as K-BLHO, were synthesized via

solid-state reactions under a high pressure using BaH_2, BaO, LiH, and KH as starting materials. A stoichiometric mixture of these materials was sealed in a pyrophyllite cell in an Ar-filled glovebox. The cell was compressed to a pressure of 2 GPa using a cubic anvil-type equipment at 650 °C for 30 min. The obtained powders were off-white colored and highly air-sensitive, hence always handled under inert atmosphere. Figure 1a shows the X-ray diffraction (XRD) patterns of the samples. Most of the reflections could be assigned to a tetragonal K_2NiF_4-type unit cell, such as that of non-doped BLHO prepared via high-pressure synthesis.[24] Figure 1b shows the calculated lattice constants at x = 0–0.3, with x = 0 corresponding to α-BLHO prepared as reported previously.[24] Negative linear correlations between the lattice constants and K content x are observed, particularly for the c-axis, indicating that the target solid solutions are successfully synthesized.

Structural analysis for the neutron diffraction (ND) pattern of the x = 0.3 sample, using a model based on α-BLHO (space group $I4/mmm$) with the Ba sites partially substituted with K atoms, converged well. A composition of $Ba_{1.7}K_{0.3}LiH_{2.5}O_{1.1}$, which is similar to the nominal composition, is observed. The fitting profiles and structural parameters are shown in Fig. S1 and Table S1, respectively, and the refined crystal structure is shown in Fig. 1c. The equatorial anion site is almost fully occupied by an H atom (H_{eq}), whereas the apical site is occupied by randomly distributed H and O atoms (H/O_{ap}) with sizable deficiencies introduced by K^+/Ba^{2+} aliovalent substitution. This trend is roughly understood according to the electrostatic valence (Pauling's second) rule that may be applied for various mixed-anion compounds with K_2NiF_4-type structures[9, 25, 26] and should contribute to the observed shrinkage in mainly the c-direction, despite the larger ionic radius of K^+ (1.55 Å) compared to that of Ba^{2+} (1.47 Å).[27] Due to Vegard's law, as shown in Fig. 1b, the K-substituted BLHO with the general formula $Ba_{2-x}K_xLiH_{2.8-x}O_{1.1}$ is also expected at x = 0.1 and 0.2.

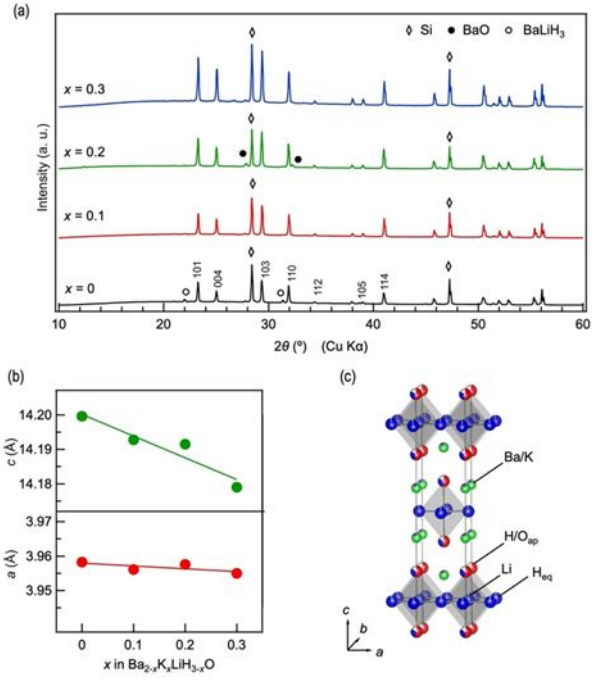

Fig. 1 (a) X-ray diffraction patterns of $Ba_{2-x}K_xLiH_{2.8-x}O_{1.1}$ (x = 0 – 0.3) synthesized via a high-pressure method. The hkl indices correspond to the tetragonal unit cell, and Si powder (SRAM 640d, National Institute of Standards and Technology, Gaithersburg, MD, USA) was used as a standard reference. Tiny amounts of BaO or $BaLiH_3$ impurity phase are observed at x = 0 or 0.2. The halo derived from the Kapton film to seal Ar gas was observed at lower angles. (b) Calculated lattice constants at x = 0 – 0.3. (c) Refined crystal structure at x = 0.3 obtained via high-pressure synthesis, as visualized using the VESTA program.[28]

When $Ba_{1.7}K_{0.3}LiH_{2.5}O_{1.1}$ (x = 0.3) was annealed at 400 °C in a H_2 atmosphere (~0.4 MPa), the tetragonal cell changed to an orthorhombic cell, which retains the K_2NiF_4-type structure, accompanied by an increased BaO content (in XRD; Fig. S2). This observation is similar to that when non-doped BLHO is used:[24] annealing $Ba_2LiH_{2.8}O_{1.1}$ (α-BLHO) under similar conditions (inert gas atmosphere with nearly ambient pressure) yields highly vacant $Ba_{1.75}LiH_{2.7}O_{0.9}$ (β-BLHO) with BaH_2 and BaO extraction. Therefore, the orthorhombic phase obtained by annealing of high-pressure synthesized K-BLHO is also expected to be a highly vacant phase via compositional change. A model based on the β-BLHO structure (space group: $Pnm2_1$) with the Ba sites partially substituted with K atoms was refined against ND data collected using the annealed sample with x = 0.3 at room temperature, yielding a good fit (Fig. S3 and Table S2). Figure 2a shows the refined structure with a composition of $Ba_{1.5}K_{0.3}LiH_{2.5}O_{0.9}$ which is considered as the stable phase at ambient temperature and pressure (β-phase) in the 15% K^+/Ba^{2+} substituted BLHO system. The three types of long-range order at the equatorial H (less/more vacancies), apical anion (H/O flipping manner), and Ba(K) sites (less/more vacancies) are similar to those in non-doped β-BLHO, except for increased structural randomness at the Ba and apical sites due to K^+/Ba^{2+} substitution.

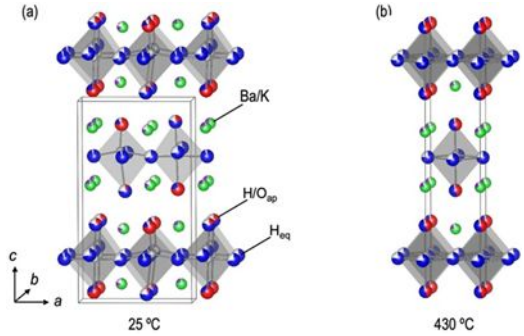

Fig. 2 Refined crystal structures of $Ba_{1.5}K_{0.3}LiH_{2.5}O_{0.9}$, which is the stable phase at x = 0.3 under ambient pressure. (a) β-phase at room temperature and (b) δ-phase at 430 °C. The crystal structures were visualized using the VESTA program.[28]

To clarify the effects of K substitution on the phase transitions in the BLHO system, temperature-controlled synchrotron XRD was performed using K-BLHO (x = 0.3) at ≤400 °C. As the measurements were carried out for α-phase ($Ba_{1.7}K_{0.3}LiH_{2.5}O_{1.1}$), transformation to the β-phase ($Ba_{1.5}K_{0.3}LiH_{2.5}O_{0.9}$) occurred at approximately 240 °C upon heating. Only the cooling profiles are shown in Fig. 3a for clarity, and all collected data are shown in Fig. S4. A structural phase transition between the orthorhombic and tetragonal phases occurs at 320 °C, which may be confirmed by the presence/absence of a superlattice peak at 2θ = 3.4° with peak separation/integration. Figure 3b shows the calculated lattice constants during cooling, along with those of the non-doped BLHO,[24] clearly revealing that the critical point of the orthorhombic-tetragonal phase transition (solid allow) is decreased by ~40 °C via 15% K^+/Ba^{2+} substitution.

The high-temperature tetragonal phase at x = 0.3 adopts a similar simple K_2NiF_4-type structure (space group: $I4/mmm$) as that of δ-BLHO,[24] as confirmed by refinement of ND data collected at 430 °C. Sizable vacancies at the Ba/K and equatorial H sites are randomly distributed, whereas few vacancies occur at the apical site. Details of the refinement are shown in Fig. S5 and Table S3. Notably, in the non-doped BLHO, another phase transition between the two orthorhombic (β- and γ-) phases is observed at 300 °C, with deviation from simple thermal expansion (dotted lines shown in Fig. 3b). Such a point occurs at approximately 240 °C in K-BLHO.

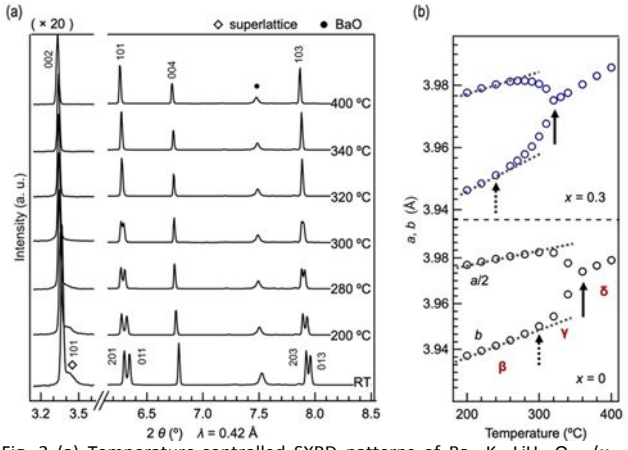

Fig. 3 (a) Temperature-controlled SXRD patterns of $Ba_{1.5}K_{0.3}LiH_{2.5}O_{0.9}$ (x = 0.3) during cooling. (b) Temperature dependences of the lattice constants, along with those of the lattice constants of the non-doped BLHO.[24] The solid arrows indicate the orthorhombic-tetragonal phase transitions, and the dotted arrows indicate deviations from linear thermal expansions of the a- and b-axes represented by the dotted lines. β, γ, and δ shown in red indicate the regions of the β-, γ-, and δ-phases, respectively.

The hydride ion conductivity of K-BLHO (x = 0.3) was evaluated via electrochemical impedance spectroscopy under H_2 atmosphere for the β-phase that is stable under ambient pressure. The pellet was prepared by sintering the α-phase at 400 °C in a H_2 atmosphere according to the results of Fig. S2. The presence of insulating BaO (~10wt.%) cannot lead to an overestimation of the conductivity of K-BLHO. Figures 4a and 4b show the impedance plots. At <250 °C, a typical semicircle attributed to the resistance of the sample (bulk and grain boundary) is observed. In contrast, at higher temperatures, only spikes due to drastic reductions in resistance are observed. Figure 4c shows the Arrhenius plot of the total conductivity (sum of bulk and grain boundary), along with those reported for representative H^- conductors of BaH_2,[8] $LaH_{2.52}O_{0.24}$,[13] and Ba_2H_3I.[17]

An increase in conductivity by >2 orders of magnitude at 240–270 °C is observed, which is a much lower temperature compared to that of the non-doped BLHO at a similar conductivity, i.e., the high conductivity region of $>10^{-3}$ S·cm^{-1} is shifted by approximately 40 °C to lower temperatures via 15% K/Ba substitution. This trend was well reproduced in a sample from a different batch even upon cycling upon 300 ºC (Fig. S6). Temperature dependences of conductivity (Fig. 4b) and lattice constants (Fig. 3b) are totally consistent in terms of a decrease in phase transition temperature (i.e. stabilization of the high conductive phase). This point indicates that the dominant charge carrier in K-BLHO is H^-, as is also the case with non-doped BLHO, wherein the pure H^- conduction was confirmed by electromotive force measurement. Note that K^+ conduction is unlikely due to its low concentration and absence of its suitable diffusion path. At 300 °C, the conductivity reached 2.0 × 10^{-2} S·cm^{-1}, which is higher than those reported for fast H^- conductors of $LaH_{2.52}O_{0.24}$ and Ba_2H_3I.

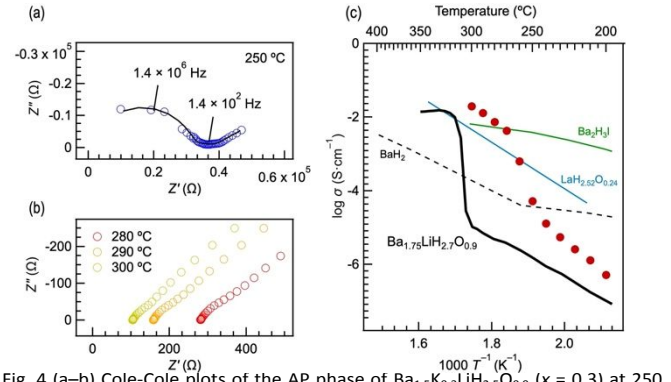

Fig. 4 (a–b) Cole-Cole plots of the AP phase of $Ba_{1.5}K_{0.3}LiH_{2.5}O_{0.9}$ (x = 0.3) at 250, 280, 290, and 300 °C. (c) Temperature dependence of the total (bulk and grain boundary contributions) conductivity (red circles), together with those of non-doped BLHO (x = 0; $Ba_{1.75}LiH_{2.7}O_{0.9}$)[24], BaH_2,[8] $LaH_{2.52}O_{0.24}$,[13] and Ba_2H_3I[17]. A comparison with other H^- conducting materials was in Fig. S9.

In our previous study based on non-doped BLHO, the drastic increase in conductivity was not accompanied by the orthorhombic (γ)–tetragonal (δ) transition at 360 °C, but by the transition between the two orthorhombic (β- and γ-) phases at 300 °C (solid and dotted allows shown in Fig. 3b).[24] In the latter, among the three types of long-range order in β-BLHO, the two at the equatorial H and Ba sites melt, with the remaining order at the apical sites forming γ-BLHO. Due to the temperature dependences of the lattice (Fig. 3b) and conductivity (Fig. 4b), such successive phase transitions are also expected in K-BLHO. The presence of the orthorhombic phase in K-BLHO corresponding to the γ-phase is suggested by the results of the refinement of the ND data of the sample with x = 0.3 collected at 270 °C (Fig. S7-S8 and Table S4-S5). Overall, the results to date indicate that K/Ba substitution in the BLHO system contributes to stabilizing the disordered (γ- and δ-) phases at lower temperatures, yielding the expanded high H^- conductivity region. It should be noted that measurements at >300 °C were challenging due to instability at K-BLHO/Mo interfaces (unknown reaction).

Conclusions

In summary, we performed aliovalent substitution of Ba^{2+} with K^+ in K_2NiF_4-type BLHO. Almost stoichiometric $Ba_{2-x}K_xLiH_{2.8-x}O_{1.1}$ (x = 0.1, 0.2, or 0.3) was obtained via high-pressure synthesis. Annealing the prepared $Ba_{1.7}K_{0.3}LiH_{2.5}O_{1.1}$ (x = 0.3) under ambient pressure yielded the vacancy-bearing $Ba_{1.5}K_{0.3}LiH_{2.5}O_{0.9}$ with the orthorhombic superlattice with three types of long-range order, corresponding to the β-phase in non-doped BLHO. The β-phase of x = 0.3 also exhibited successive phase transitions to the orthorhombic γ-phase and then the

tetragonal δ-phase, but the critical temperatures were decreased by approximately 50 °C compared to those observed for the non-doped material. Stabilization of the high-temperature γ- and δ-phases contributed to the expansion of the high conductivity region to lower temperatures. Therefore, the stabilization of a high-temperature phase by introducing structural randomness may also be applied to the fast H^- conductor BLHO, and further improvement via the optimization of the compositions at the other sites is expected. In addition, elucidation of the conductive behavior of the tetragonal δ-phase of the BLHO system remains necessary. Further investigation, e.g., the appropriate design of stable electrode/electrolyte interfaces for use in electrochemical measurements at high temperatures combined with a dynamics study using various methods, such as quasi-elastic neutron scattering, nuclear magnetic resonance spectroscopy, and molecular dynamics simulation, is required.

This work was supported by the following grants: Japan Science and Technology Agency (JST) FOREST (JPMJFR213H), Grant-in-Aid for Scientific Research (19K12650, 20H02828, 22K14755), Scientific Research on Innovative Areas (17H05492, 18H05516, 18H05518, 19H04710, 22H04514), and Challenging Research (22K18909) from the Japan Society for the Promotion of Science. The synchrotron and neutron radiation studies were approved by the Japan Synchrotron Radiation Research Institute (2018B1099, 2019A1084, 2020A1659) and the Neutron Scattering Program Advisory Committee of the Institute of Materials Structure Science, High Energy Accelerator Research Organization (2019S10).

Conflicts of interest

There are no conflicts to declare.

Notes and references

1. C. Tubandt and E. Lorenz, *Z. Phys. Chem.*, 1914, **87**, 513.
2. J. B. Goodenough, J. E. Ruizdiaz and Y. S. Zhen, *Solid State Ionics*, 1990, **44**, 21-31.
3. B. B. Owens and G. R. Argue, *Science*, 1967, **157**, 308-310.
4. K. Shahi and J. B. Wagner, *J. Phys. Chem. Solids*, 1982, **43**, 713-722.
5. K. Kakinuma, H. Yamamura, H. Haneda and T. Atake, *Solid State Ionics*, 2001, **140**, 301-306.
6. T. Yao, Y. Uchimoto, M. Kinuhata, T. Inagaki and H. Yoshida, *Solid State Ionics*, 2000, **132**, 189-198.
7. M. C. Verbraeken, E. Suard and J. T. S. Irvine, *J. Mater. Chem.*, 2009, **19**, 2766-2770.
8. M. C. Verbraeken, C. Cheung, E. Suard and J. T. Irvine, *Nat. Mater.*, 2015, **14**, 95-100.
9. G. Kobayashi, Y. Hinuma, S. Matsuoka, A. Watanabe, M. Iqbal, M. Hirayama, M. Yonemura, T. Kamiyama, I. Tanaka and R. Kanno, *Science*, 2016, **351**, 1314-1317.
10. Y. Iwasaki, N. Matsui, K. Suzuki, Y. Hinuma, M. Yonemura, G. Kobayashi, M. Hirayama, I. Tanaka and R. Kanno, *J. Mater. Chem. A*, 2018, **6**, 23457-23463.
11. F. Takeiri, A. Watanabe, A. Kuwabara, H. Nawaz, N. I. P. Ayu, M. Yonemura, R. Kanno and G. Kobayashi, *Inorg. Chem.*, 2019, **58**, 4431-4436.
12. H. Nawaz, F. Takeiri, A. Kuwabara, M. Yonemura and G. Kobayashi, *Chem. Commun.*, 2020, **56**, 10373-10376.
13. K. Fukui, S. Iimura, T. Tada, S. Fujitsu, M. Sasase, H. Tamatsukuri, T. Honda, K. Ikeda, T. Otomo and H. Hosono, *Nat. Commun.*, 2019, **10**, 2578.
14. H. Ubukata, T. Broux, F. Takeiri, K. Shitara, H. Yamashita, A. Kuwabara, G. Kobayashi and H. Kageyama, *Chem. Mater.*, 2019, **31**, 7360-7366.
15. K. Fukui, S. Iimura, A. Iskandarov, T. Tada and H. Hosono, *J. Am. Chem. Soc.*, 2022, **144**, 1523-1527.
16. A. Iskandarov, T. Tada, S. Iimura and H. Hosono, *Acta Mater.*, 2022, **230**.
17. H. Ubukata, F. Takeiri, K. Shitara, C. Tassel, T. Saito, T. Kamiyama, T. Broux, A. Kuwabara, G. Kobayashi and H. Kageyama, *Sci Adv*, 2021, **7**, eabf7883.
18. H. Ubukata, F. Takeiri, C. Tassel, S. Kobayashi, S. Kawaguchi, T. Saito, T. Kamiyama, S. Kobayashi, G. Kobayashi and H. Kageyama, *Chem. Mater.*, 2022.
19. T. Hirose, T. Mishina, N. Matsui, K. Suzuki, T. Saito, T. Kamiyama, M. Hirayama and R. Kanno, *ACS Appl. Energy Mater.*, 2022, **5**, 2968-2974.
20. X. Liu, T. S. Bjørheim and R. Haugsrud, *J. Mater. Chem. A*, 2018, **6**, 1454-1461.
21. Q. Bai, X. He, Y. Zhu and Y. Mo, *ACS Appl. Energy Mater.*, 2018, **1**, 1626-1634.
22. H. W. T. Morgan, H. J. Stroud and N. L. Allan, *Chem. Mater.*, 2021, **33**, 177-185.
23. O. S. Fjellvag, J. Armstrong, P. Vajeeston and A. O. Sjastad, *J. Phys. Chem. Lett.*, 2018, **9**, 353-358.
24. F. Takeiri, A. Watanabe, K. Okamoto, D. Bresser, S. Lyonnard, B. Frick, A. Ali, Y. Imai, M. Nishikawa, M. Yonemura, T. Saito, K. Ikeda, T. Otomo, T. Kamiyama, R. Kanno and G. Kobayashi, *Nat. Mater.*, 2022, **21**, 325-330.
25. A. Fuertes, *Inorganic Chemistry*, 2006, **45**, 9640-9642.
26. K. Wissel, J. Heldt, P. B. Groszewicz, S. Dasgupta, H. Breitzke, M. Donzelli, A. I. Waidha, A. D. Fortes, J. Rohrer, P. R. Slater, G. Buntkowsky and O. Clemens, *Inorg. Chem.*, 2018, **57**, 6549-6560.
27. R. D. SHANNON, *Acta Crystallogr. Section A*, 1976, **32**, 751-767.
28. K. Momma and F. Izumi, *J. Appl. Crystallogr.*, 2011, **44**, 1272-1276.